PAPER

Synergistic regulation of cerebellar Purkinje neuron development by laminin epitopes and collagen on an artificial hybrid matrix construct†

Shantanu Sur,[a,b,c] Mustafa O. Guler,[c,d] Matthew J. Webber,[e] Eugene T. Pashuck,[f] Masao Ito,[a] Samuel I. Stupp[c,e,f,g] and Thomas Launey*[a,h]

The extracellular matrix (ECM) creates a dynamic environment around the cells in the developing central nervous system, providing them with the necessary biochemical and biophysical signals. Although the functions of many ECM molecules in neuronal development have been individually studied in detail, the combinatorial effects of multiple ECM components are not well characterized. Here we demonstrate that the expression of collagen and laminin-1 (lam-1) are spatially and temporally correlated during embryonic and post-natal development of the cerebellum. These changes in ECM distribution correspond to specific stages of Purkinje neuron (PC) migration, somatic monolayer formation and polarization. To clarify the respective roles of these ECM molecules on PC development, we cultured cerebellar neurons on a hybrid matrix comprised of collagen and a synthetic peptide amphiphile nanofiber bearing a potent lam-1 derived bioactive IKVAV peptide epitope. By systematically varying the concentration and ratio of collagen and the laminin epitope in the matrix, we could demonstrate a synergistic relationship between these two ECM components in controlling multiple aspects of PC maturation. An optimal ratio of collagen and IKVAV in the matrix was found to promote maximal PC survival and dendrite growth, while dendrite penetration into the matrix was enhanced by a high IKVAV to collagen ratio. In addition, the laminin epitope was found to guide PC axon development. By combining our observations *in vivo* and *in vitro*, we propose a model of PC development where the synergistic effects of collagen and lam-1 play a key role in migration, polarization and morphological maturation of PCs.

Introduction

The extracellular matrix (ECM) microenvironment plays a critical role in tissue development through dynamic temporal and spatial control of cell signaling.[1] In the nervous system, it governs neuronal differentiation, migration, neurite outgrowth, and synaptogenesis.[2–5] Specifically, during the development of the cerebellum, several ECM components are expressed transiently and are confined to specific regions. For example, fibronectin is expressed along the migration route of granule cell (GC) precursors during the second embryonic week and facilitates cell movement from the rhombic lip to the external germinal layer (EGL).[6] Similarly, interaction of vitronectin with $\alpha_v\beta_5$ integrin receptors in the early post-natal period supports the elongation of GC axons,[7] while transient perinatal expression of reelin by EGL neurons is critical for the proper alignment of Purkinje neurons (PCs).[8]

Laminin-1 (lam-1) is an ECM molecule that plays a prominent role in the development of various tissues,[9] and is also expressed transiently in the perinatal cerebellum.[10] Previous *in vitro* studies have shown that lam-1 promotes cerebellar GC migration and neurite outgrowth[10,11] and facilitates sprouting of the PC spine.[12] Conditional knock-out of the laminin α1 chain from lam-1 resulted in reduced proliferation of GC precursors, disorganization in Bergman glial processes, reduced PC dendrite growth, and disruption of PC arrangement in the cerebral cortex.[13] Similarly, microarray analysis at different developmental stages has shown that several forms of fibrillar

ᵃLaboratory for Memory and Learning, Wako-shi, 351-0198 Saitama, Japan
ᵇSchool of Medical Science and Technology, IIT Kharagpur, 721302, India
ᶜThe Institute for Bionanotechnology in Medicine (IBNAM), Northwestern University, Chicago, IL 60611, USA
ᵈInstitute of Materials Science and Nanotechnology, National Nanotechnology Research Center (UNAM), Bilkent University, Ankara, 06800, Turkey
ᵉDepartment of Biomedical Engineering, Evanston, IL 60208, USA
ᶠDepartment of Materials Science and Engineering, Evanston, IL 60208, USA
ᵍDepartment of Chemistry, Northwestern University, Evanston, IL 60208, USA
ʰLauney Research Unit for Molecular Neurocybernetics, RIKEN Brain Science Institute, Wako-shi, 351-0198 Saitama, Japan. E-mail: t_launey@brain.riken.jp; Fax: +81 48 462 4697; Tel: +81 48 462 1613
†Electronic supplementary information (ESI) available. See DOI: 10.1039/c3bm60228a

collagen, including types I, II, III, and V are transiently expressed in the developing cerebellum (Cerebellar Development Transcriptome Database, CDT-DB[14]), and their levels sharply decrease by the end of the third postnatal week when the cerebellum reaches maturity. Indications of temporal overlap of collagen and laminin expression in the developing cerebellum, along with previous reports of their correlated co-expression during neural crest development,[15] raise the possibility of functional cooperation between these two ECM components to control cerebellar development. Regulation of tissue development through combinatorial signaling from multiple ECM components has been demonstrated *in vitro*;[16] different ECM molecules may interact by influencing structure[17] or through cross-talk at the integrin signaling level.[18] However, little is known regarding the spatial and temporal association of laminins and collagens within the developing cerebellar tissue and the potential synergies that result from co-localized signaling of these two ECM components.

In this work, first we investigated the spatiotemporal pattern of both lam-1 and collagens expressions during cerebellar development. We then explored the relationship between the distribution of these two ECM components and the migration and maturation of PCs as they organize into a dense monolayer of neurons with highly polarized dendrites. To investigate the causal relationship between the observed ECM changes and PC patterning, we developed an artificial matrix comprised of collagen and a synthetic fibrillar material presenting a potent lam-1 derived epitope. This controlled substrate allowed us to evaluate the functional relationship between collagen and lam-1 *in vitro* and their relative contributions to different aspects of PC development.

Experimental

Hybrid matrix preparation

The hybrid matrix was prepared as described previously.[19] Briefly, branched peptide amphiphile (PA) molecules were synthesized using solid-phase peptide synthesis (SPPS) methods.[20] Fmoc-protected amino acids, MBHA rink amide resin, and HBTU were purchased from NovaBiochem (USA) and all other reagents for synthesis were purchased from Fisher (USA) or Sigma-Aldrich (USA). PA stock solutions (1% w/v in water, pH 4) were stored at −80 °C, and sonicated in a water bath for 20 min before use. Type I collagen was extracted from Wistar rat tail (3–4 month old), following the method of Chandrakasan *et al.*,[21] with some modifications. In brief, the collected tendons were dissolved in 0.1 M acetic acid and purified by centrifugation and repeated dialysis (molecular weight cutoff 10 kDa) to remove insoluble materials and small molecular weight contaminants. The purified sample was finally dialyzed against 0.1X DMEM solution or 5 mM pyruvic acid (both adjusted to pH 4) and stored at −80 °C. Purity of collagen was confirmed by SDS-PAGE electrophoresis and concentration was estimated using EZQ protein quantification kit (Molecular Probes, Inc.) and measurement of dry weight after lyophilization.

Immediately before preparing the gel, collagen and PA stock solutions were diluted in sterile MilliQ water to the appropriate working concentration, mixed quickly and 50 μL of the mixed solution was spread in a glass bottomed well (8 mm diameter) at the centre of 35 mm Petri dish (Falcon 3001). Gelation of the mixed solution was induced by exposure to ammonia vapour for 10 minutes at room temperature. 100 μL DMEM solution was added on top of the gel and left overnight in an incubator at 37 °C and 5% CO_2 for buffer exchange and to ensure stable supramolecular gel formation.

Rheology

Rheological measurements were performed on a Paar Physica MCR 300 oscillating plate rheometer using a 25 mm diameter cone-plate geometry and a gap of 0.05 mm. The collagen (type I from rat tail, BD bioscience) and PA solutions were maintained at 4 °C, and mixed at the desired concentration immediately before each measurement. The mixture of collagen and PA was then quickly pipetted (175 μL) onto the rheometer plate and gelled by exposure to ammonia vapor for 20 min at 25 °C. All measurements were done at 25 °C, and the gels were allowed to equilibrate for 5 min at 0.1% strain prior to measurement. Data were collected at 0.1% strain over a frequency range of 1 to 100 s^{-1} and traces from three separate runs were averaged for each condition.

Cerebellar culture

Dissociated mixed cerebellar cultures were prepared from 18 day rat (Wistar) embryos, following established protocols.[19,22] Briefly, the cerebella were dissected out from embryos in ice cold Ca^{2+}/Mg^{2+}-free Hank's balanced salt solution (HBSS), and were sequentially treated with 0.25% trypsin in HBSS for 20 min at room temperature, followed by 0.05% DNase in HBSS supplemented with 5% horse serum and 12 mM $MgSO_4$, for 3 min at 4 °C. Trypsin digested cerebella were dissociated into single cells by mechanical trituration with a fire-polished Pasteur pipette. Viable cell fraction was recovered from the cell suspension by centrifuging at 3000*g* for 15 min over a 10 and 60% percoll column and collecting cells from the 10–60% interface. The cells were re-suspended in seeding medium containing DMEM F-12 and 10% heat inactivated Horse serum. The cell suspension was seeded on preformed gels at a concentration of 4800 cells mm^{-2} and after 2 h, 1 mL of culture medium was added with composition as described by Sur *et al.*[19] For long-term cultures, half of the medium was replaced on the 14th day and every 7th day thereafter. All saline solutions were obtained from Gibco BRL Life Tech (Tokyo, Japan) and the reagents and enzymes were purchased from Sigma (Tokyo, Japan). Dissection and animal handling were carried out in accordance with the National Institutes of Health Guide for the Care and Use of Laboratory Animals, and specifically approved by the Research Ethics Section of the RIKEN institute.

Culture immunostaining

Cultured cells were fixed with 4% paraformaldehyde in 0.1 M PBS (pH 7.4) at room temperature (RT) for 15 min. Fixed cells were permeabilized and blocked against nonspecific protein binding (10% normal goat serum, 2% bovine serum albumin and 0.4% Triton X-100 in PBS) for 30 min at RT. The following primary antibodies were used (with specified dilution) for immunodetection: mouse anti-neuronal nuclei (NeuN) monoclonal (1 : 500, Chemicon International, USA); mouse anti-tubulin, beta III isoform monoclonal (1 : 1000, Chemicon); anti-calbindin D-28k (mouse monoclonal, 1 : 1000, Swant, Bellinzona, Switzerland and rabbit polyclonal, 1 : 1000, Chemicon); mouse anti-synaptophysin monoclonal (1 : 10 000, Chemicon). The primary antibodies were incubated overnight at 4 °C for binding, and then detected with the appropriate Alexa-conjugated secondary antibodies (Molecular Probes, Inc., 2 h incubation at RT). Actin was visualized by Alexa Fluor 594 conjugated phalloidin (1 : 1000, Invitrogen, USA).

Slice immunostaining

Postnatal Wistar rat cerebellums (P1–21) were fixed by transcardiac perfusion of 4% paraformaldehyde (PFA) in PBS (pH 7.4). Cerebellum was dissected and post-fixed in the same solution overnight at 4 °C. For the embryonic cerebella (E18–20), the brains were first dissected in ice cold HBSS and then fixed by exposure to 4% PFA in PBS for 24 hours. The fixed samples were sequentially incubated in 10%, 20% and 30% sucrose solution (w/v), before embedding in the O.C.T. medium (Tissue Tek®, Sakura Finetek Co. Ltd, Japan) by quick freezing. Sagittal cerebellar sections (20 μm thick) were prepared from the frozen tissue block using a Leica 3050 cryostat. Sections were permeabilized and blocked with 10% normal goat serum, 2% bovine serum albumin and 0.4% Triton X-100 in PBS for 30 min at RT. For primary antibody binding, samples were incubated in antibody solution overnight at 4 °C. Rat anti-laminin-1 polyclonal antibody (1 : 1000, Chemicon) was used to detect lam-1 expression and rabbit polyclonal anti-collagen antibodies (all from Abcam, UK) to type I–V (ab36064, 1 : 200, Abcam, UK), type I (ab59435, 1 : 500), type II (ab116242, 1 : 500) and IV (ab19808, 1 : 500) were used to detect collagen expression. PC and GC populations were detected using the same antibody and dilution as used for culture. The slices were then washed in PBS three times, and incubated in Alexa-conjugated secondary antibodies for 1 hour.

Image acquisition and analysis

Fluorescence stained cultures/tissue sections were imaged either through a cooled CCD camera (Coolsnap Photometrics, Tucson, AZ) attached to an upright microscope (BX51, Olympus) or by using confocal laser scanning microscope (FV500 and FV1000, Olympus). To quantify PC surface dendritic growth, the PC projected surface area and convex hull were estimated. In order to exclude the substrate-penetrating branches, only the upper 20 μm of confocal stacks were considered for the measurement. The stacks were projected and

thresholded—the area covered by a single PC soma and its dendrites was considered as projected surface area. The convex hull (an index of PC dendritic spread on the substrate) was defined as the total area obtained by joining the most distal dendritic tips with straight lines. The analysis was done semi-automatically using routines written in Matlab and ImageJ (NIH). Deconvolution of the confocal image stacks was done using Huygens software (Scientific Volume Imaging, Netherlands).

Statistical analysis

A nonparametric method (Mann Whitney U test) was used for paired comparison between data-groups. Bargraph represents mean ± SEM.

Results

Spatiotemporal expression of lam-1 and collagen in perinatal cerebellum

We first examined the distribution of lam-1 and collagens in the cerebellar tissue and their association to developing PCs during the perinatal period beginning at embryonic day-18 (E18) and continued to post-natal day-21 (P21). This timeframe coincides with the period of PC cortical migration and morphological maturation.[23] Comparisons between developmental stages were made at the (future) lobule V/VI of cerebellar vermis to avoid the region-specific variability in the temporal course of PC development.[24] Lam-1 was strongly expressed (detected with an antibody against the laminin α1 chain) around the blood vessel and meningeal membranes (Fig. 1A), as the basement membrane is a rich source of laminin.[13] In addition, an apparent concentration gradient of the protein was evident in the E18 cerebellum, decreasing across the vermis from the ventricle to the cortical surface. This gradient was even more prominent in subsequent days (P1) as the cerebellum rapidly enlarged and formed lobules. Concomitant change in the distribution of PCs was visualized by staining for PC specific protein calbindin D28k. At E18, PC somas were distributed over the entire vermis, with a higher density near the posterior lobule through which they enter the cerebellum.[24] In addition, the trailing boundary of these peripherally migrating PCs was remarkably well correlated with an abrupt decrease in lam-1 expression (Fig. 1A; E18, P1). The PCs eventually settled in a narrow band below the external germinal layer (EGL), which is densely packed with immature GCs, stained by antibody against neuron-specific nuclear protein (NeuN).[25] In contrast to the somatic migration pattern, the axons of these PCs elongated deeper into the laminin-rich regions of the cerebellum (Fig. 1A; P1). NeuN-positive GCs were found to migrate in the opposite direction during this period (from EGL to the deeper cortex) and form the future internal granular layer (IGL). These observations suggest that the lam-1 gradient may provide cues for the migration of the PCs and the direction of the axon growth.
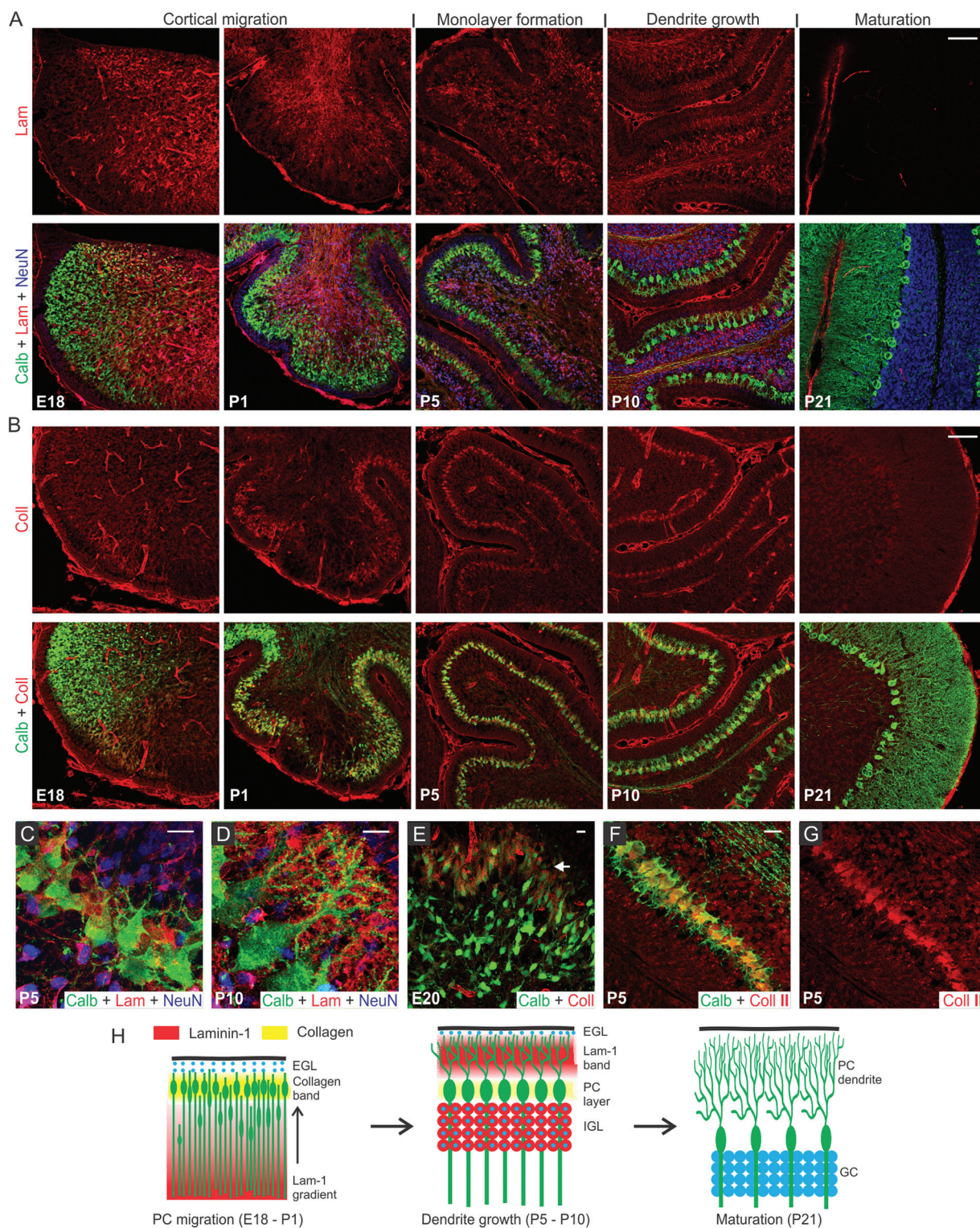
Fig. 1 Spatio-temporal expression of lam-1 and collagen in the cerebellum during PC development. (A) Lam-1 stained sections of rat cerebellar vermis, at selected time-points between embryonic 18 days (E18) and post-natal 21 days (P21) (*top row*). PC and GC distribution in the corresponding sections is shown by co-immunostaining against calbindin (green) and NeuN (blue), respectively (*bottom row*). (B) Collagen (type I–V) distribution in the vermis at the time-points shown in A (*top row*), and its relationship to the developing PCs (*bottom row*). Magnified view of the PC layer at P5 (C) and P10 (D) shows the spatial association of lam-1 with PC soma and dendrites. (E) Higher collagen expression (arrow) was observed around the peripherally distributed PCs at E20. (F) Spatial association of PCs and collagen II expression at P5. The collagen II channel is shown separately in (G). (H) Schematic illustration of the association of collagen and lam-1 during cerebellar development and PC morphogenesis (EGL, external germinal layer; IGL, internal granular layer). Scale bars (micron) A,B, 100; C,D,E, 10; F, 20.

By P5, the monolayer alignment of PC soma was almost complete and the lam-1 gradient disappeared. At this time, a majority of the GCs also migrated from the EGL to internal granular layer (IGL), and lam-1 was only focally expressed around the GC soma (Fig. 1A and C). In addition, weak lam-1 expression was also found around the PCs, which have a typical "stellate" shape with multiple short dendrites radiating in all directions from the soma. By P10, the lam-1 expression shifted peripherally, with a distinct stripe of lam-1 occupying the lower part of the newly formed molecular layer (Fig. 1A and D). The supernumerary dendrites of the PCs had retracted at this stage, and a single primary dendrite arising from the cortical side of the soma extended and branched extensively within the molecular layer. The dendritic extension, however, was restricted within the outer boundary of this lam-1 stripe. In addition, PC soma and dendrites did not show any intracellular lam-1 staining, as has been reported before for laminin-2 at this stage of development.[10] From P21 through the adult stage, lam-1 was not detectable anywhere throughout the cerebellar tissue.

To examine the spatiotemporal expression of collagen, we used a wide-specificity collagen antibody to detect all common fibrous subtypes (type I, II, III, V) as well as basement membrane (IV) collagen. Similar to lam-1, collagen also demonstrated a very specific distribution pattern at the various timepoints during development, though the pattern for collagen was very different from that of lam-1. In the E18 cerebellum, high levels of collagen expression were found only within the basement membrane of blood vessels and the meningeal surface (Fig. 1B). However, by P1 a prominent band of collagen had developed in the cerebellar cortex located beneath the EGL. This band of collagen spatially coincides with the layer of migrating PCs (Fig. 1B and E). As PCs became organized and aligned, the corresponding band of collagen became thinner and its width at P5 corresponded to the width of the PC soma monolayer (Fig. 1B, P5). This collagen band was still present at P10 and remained spatially associated with the PC soma during the dendritic sprouting, but was undetectable at P21. Collagen expression in the PC soma layer is especially remarkable, as no similar banding was observed in the cerebral cortex (Fig. S1†). To determine the subtype of the expressed collagen, sections were stained with antibodies specific for collagen type I, type II and type IV. We observed that type II collagen was distributed along the PC layer, similar to what we observed with the broad spectrum collagen antibody (Fig. 1F and G). Collagen type I and type IV distributions, however, were confined to the blood vessel wall and meningeal membranes only (Fig. S2†). Type II specificity of the collagen in PC layer is not completely unexpected, since its expression has been reported in several regions of the developing mouse brain and procollagen IIA has been shown to be critical for the forebrain development.[26,27]

PC survival at different collagen to lam-1 epitope ratios *in vitro*

The dynamic spatiotemporal expression of lam-1 and collagen in the developing cerebellum (summarized in Fig. 1H),

combined with their absence in the adult tissue, suggests the involvement of these ECM proteins in directing the formation of the cerebellar neural architecture. Moreover, the overlap in their distribution near PCs suggests potential cooperative signaling to control the development of these neurons. This possible cooperativity was explored using an *in vitro* model system, which was based on our previously reported hybrid matrix platform that incorporates collagen along with a potent laminin-specific epitope.[19] As there are difficulties to obtain a homogeneous mixing of laminin and collagen *in vitro*,[28] the laminin component of this hybrid matrix was represented using fibrillar nanostructures composed of peptide amphiphile (PA) molecules that present a lam-1-derived bioactive epitope, IKVAV.[29,30] PA nanostructures have been extensively studied in recent years as a platform to present bioactive signals[31–34] to cells. The design of PA molecules used here includes a short hydrophilic peptide sequence conjugated to a hydrophobic palmitoyl tail. The amphiphilic character of the PA molecules drives their self-assembly into nanofibers at physiological pH and salt concentrations. The hydrophobic components collapse into the nanofiber core and β-sheet hydrogen bonding occurs between residues adjacent to the tail in order to promote the formation of high aspect ratio one dimensional filamentous assemblies of hundreds of nanometers to microns in length.[35] The incorporation of bioactive epitopes on the end of the molecule opposite to the hydrophobic tail facilitates epitope display at high density on the surface of the assembled high aspect-ratio nanofibers.[30] A branched molecular architecture in the peptide domain of the PA molecule, such as the structure of the IKVAV-PA used to construct the hybrid matrices here (Fig. 2A), enables enhanced epitope spacing in the assembled nanofibers and improves receptor accessibility.[36,37] The IKVAV epitope is responsible for a large fraction of the bioactivity of lam-1 on neuronal attachment, differentiation and neurite growth[29,30,38] but the attachment of the epitopes to a scaffold is necessary to initiate cell response.[19]

For the collagen component of the hybrid matrix, type II collagen would have been ideal as this collagen subtype was observed in the developing cerebellum. However, there is little literature precedent using collagen type II as a scaffold, except to deliver chondrogenic cells *in vivo*.[39] Isolation of type II collagen requires pepsin digestion and removal of the telopeptide region from the collagen molecule.[40] This may lead to the formation of a weaker gel,[41] and thus is not desirable for an *in vitro* scaffold. Our attempts to prepare a hybrid matrix using commercially available collagen type II yielded gels that were not strong enough to perform cell experiments. Therefore, type I collagen was chosen as the collagen component of this hybrid matrix because it is structurally similar to the fibrillar type II isoform, can be easily purified from rat tail without pepsin-digestion, and forms a robust gel when mixed with PA. This enabled a tunable hybrid matrix, prepared from IKVAV-PA and type I collagen, as a well-defined substrate to evaluate the cooperative effects of collagen and lam-1 on PC development *in vitro*.
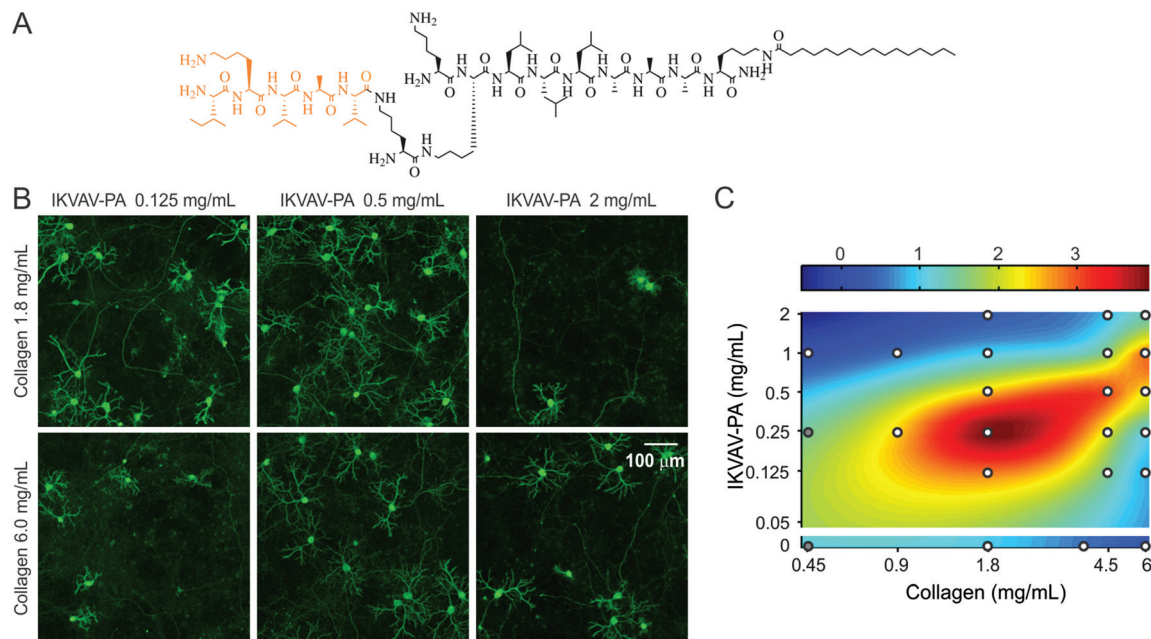
Fig. 2 Effects of collagen IKVAV-PA hybrid matrix composition on PC density. (A) Chemical structure of IKVAV-PA molecule. (B) Cerebellar cultures (16 days *in vitro*) on hybrid matrices with different collagen and IKVAV-PA concentrations, stained for calbindin to visualize PCs. (C) 2D color map representation of PC density on hybrid matrix of varying collagen and PA concentrations (all replicates normalized to the PC density on a matrix of collagen 1.8 mg mL^{-1} and IKVAV-PA 1 mg mL^{-1}). White circles represent the sampling points (average of ≥40 random fields from 2–4 culture plates). At compositions indicated by the gray circles matrices were too soft to manipulate for staining but neuron density was drastically reduced.

This collagen-PA hybrid matrix forms a robust gel and allows the concentration of both collagen and the IKVAV epitope to be varied over a broad range in order to study the effects of altered matrix composition on cultured neurons. For example, we have previously demonstrated that changing the IKVAV epitope content, while maintaining constant collagen concentration, can be used to control PC survival and morphogenesis.[19] To evaluate whether the collagen component contributes to a change in PC number, we compared cultures on two collagen concentrations (1.8 and 6.0 mg mL^{-1}) in the presence of a range of IKVAV epitope contents (Fig. 2B). PC response to IKVAV epitopes in the matrix was found to be highly dependent on the collagen concentration. At higher IKVAV PA concentration (2.0 mg mL^{-1}), the PC density was low in the presence of 1.8 mg mL^{-1} collagen, but the number was partially recovered when the collagen concentration was increased to 6.0 mg mL^{-1}. In contrast, at a lower IKVAV PA concentration (0.125 mg mL^{-1}) the response was opposite, with higher PC survival observed in the case of lower collagen content. To examine the complex nature of the collagen–IKVAV PA interaction, we measured PC density in two weeks old culture for 21 distinct matrix compositions, where collagen and IKVAV PA concentrations were systematically varied over a range of 0.45–6.0 mg mL^{-1} and 0–2.0 mg mL^{-1}, respectively. A biharmonic spline interpolation through these sampled points revealed that the matrix compositions associated with high PC density were located along a diagonal ridge (Fig. 2C). This implies that for a given collagen concentration, there exists an optimal range of IKVAV, as previously reported.[19]

However, the optimal IKVAV content was also dependent on collagen concentration, exemplified by the shift in the peak survival from 0.25 mg mL^{-1} IKVAV PA to 1.0 mg mL^{-1} IKVAV PA that was observed when collagen concentration was changed from 1.8 mg mL^{-1} to 6.0 mg mL^{-1}. Using either collagen or IKVAV-PA gel alone at high concentration (6 mg mL^{-1} for collagen or 5 mg mL^{-1} for IKVAV-PA, minimum PA concentration required to form a self-supporting gel) resulted in very low PC density, suggesting that the single component matrices were less favorable for PC survival at high concentrations (Fig. 2C). Interestingly, on the hybrid matrix at a high concentration of both components, improved PC density was observed. Taken together, these results suggest that the critical factor for PC survival is the Collagen/IKVAV PA ratio in these hybrid matrices, rather than the absolute concentration of either component.

IKVAV epitope and PC axon guidance

We observed that in the developing cerebellum, PC axons extend towards the lam-1 rich region. Therefore, we explored whether the IKVAV epitope could similarly guide PC axons when grown on our hybrid matrix. To test this, we prepared collagen gel (1.8 mg mL^{-1}) side-by-side with a hybrid gel including IKVAV PA (2 mg mL^{-1}) in the same culture well (Fig. 3A). The weak auto-fluorescence from the IKVAV PA allowed the detection of the interface between the two gels by confocal microscopy (Fig. 3B; red channel) and confirmed that there was minimal diffusion of IKVAV PA into the collagen compartment. When cerebellar cells were cultured on this
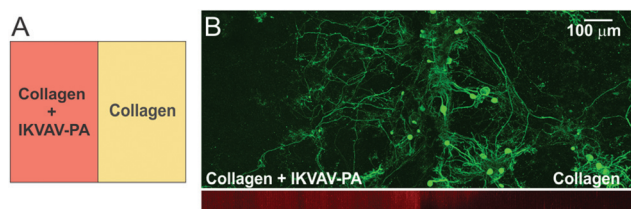
Fig. 3 PC axon growth on IKVAV epitope rich substrate. (A) Gel design for the experiment: half of the gel was made up of hybrid matrix (collagen 1.8 mg mL^{-1}, IKVAV-PA 2 mg mL^{-1}) and the rest contained collagen only. (B) *Bottom image*: two gel regions could be distinguished by weak red auto-fluorescence from the PA molecules (side view from a confocal stack). *Top image*: distribution of PC (calbindin+) soma and axons cultured on this substrate for 4 weeks.

matrix, PC somas were mostly distributed on the collagen side, close to the interface of the two compartments (Fig. 3B). This clustering of PC soma near the interface can be explained by our previous finding that PC survival is higher at certain ratios of collagen and IKVAV PA, with the optimal ratio being present near the interface from some diffusion of PA. However, the axons of these PCs predominantly crossed the interface and extended into the IKVAV-rich region, suggesting that IKVAV epitopes served as an attracting cue to the developing PC axons. This supports evidence that biological signaling arising from the sharp lam-1 gradients, such as those observed *in vivo* and recreated using our hybrid matrix, could be responsible for guiding the extension of PC axons toward the deeper region of the cerebellum during development.

Collagen and IKVAV on PC dendrite maturation

As we observed accumulation of lam-1 around the growing dendrites at P10, we next evaluated whether the composition of the hybrid matrix could similarly control PC dendrite morphogenesis *in vitro*. On our 3D hybrid matrix, PCs may exhibit two modes of dendrite growth: surface growth at the gel-culture medium interface and substrate-penetrating growth into the matrix.[19] At a collagen concentration of 1.8 mg mL^{-1}, the maximal surface dendritic growth was seen with low IKVAV-PA concentrations (0.25 mg mL^{-1}), and the growth was markedly reduced as PA concentration was increased to 2 mg mL^{-1} (Fig. 4A). Surface dendrite growth was also highly dependent on the collagen concentration in the matrix, as an IKVAV-PA concentration of 1 mg mL^{-1} allowed the formation of only very short surface dendrites at a collagen concentration of 0.45 mg mL^{-1}, but extensive growth was observed when the collagen concentration was 6.0 mg mL^{-1}. In contrast, substrate-penetrating dendritic growth was favored when the PA concentration in the matrix was increased (Fig. 4A). To quantify the surface dendritic growth, projected surface area and convex hull were measured following the methods described previously.[19] The average surface area and convex hull on low-collagen hybrid matrix (collagen 0.45 mg mL^{-1}, IKVAV PA 1 mg mL^{-1}) were 975 ± 49 μm^2 and 2182 ± 189 μm^2, respectively, corresponding essentially to the surface of the soma and a few
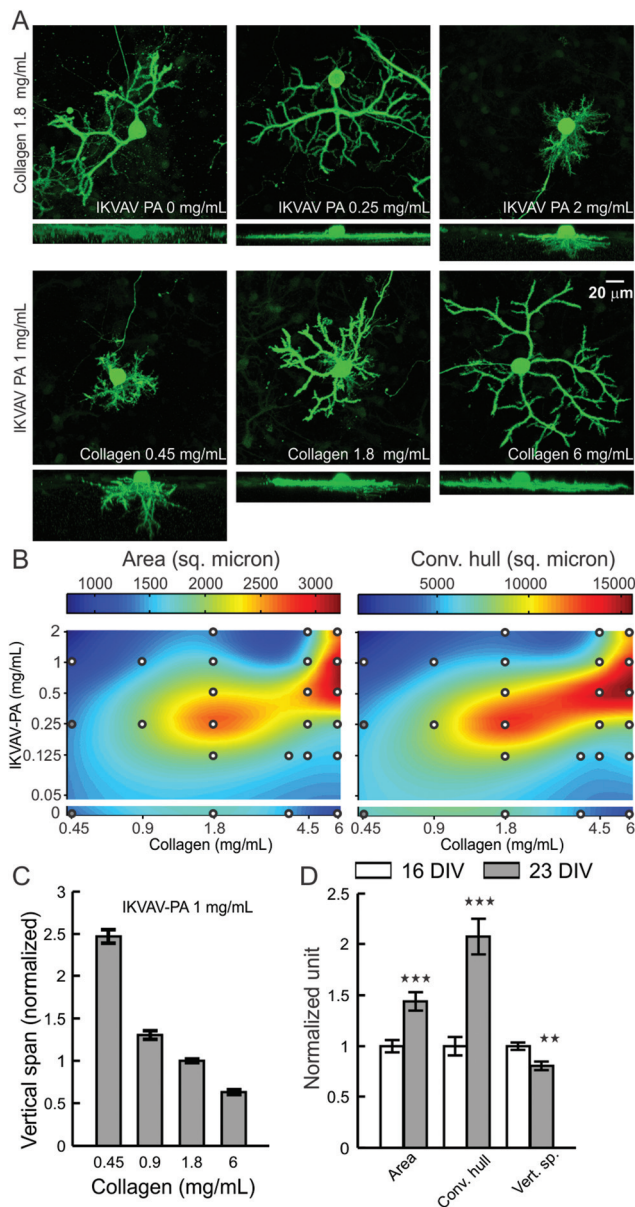

Fig. 4 Effects of collagen and IKVAV-PA concentration on PC dendrite morphology. (A) Representative images of PCs (calbindin+), cultured for 16 days on hybrid matrix with different concentrations of collagen and PA. For each condition, the upper image shows top projection, and the lower image shows side projection from a confocal image stack. (B) Colormap representation of the area and convex hull of PC surface dendrites on hybrid matrices with a range of collagen and PA concentration. White circles indicate the sampling points (each point represents an average of 18–71 PCs); at compositions marked by gray circles the matrix became too soft to sustain the staining and imaging procedure. (C) Vertical span of PCs are plotted against the collagen concentration in hybrid matrix ($n \geq 28$ PCs for each concentration). (D) Temporal change in PC dendrite morphology on hybrid matrix (collagen 1.8 mg mL^{-1}, IKVAV-PA 1 mg mL^{-1}) after 16 and 23 days of culture (**: $p < 0.01$, ***: $p < 0.001$, $n > 50$ PCs).

short dendrites. These values increased by 231 ± 16% and 554 ± 41%, respectively, for matrices prepared with 6 mg mL^{-1} collagen (at constant IKVAV PA concentration). This trend in

surface growth was not displayed when the matrix was made of pure collagen, as PC surface area decreased by 39 ± 6% for 6 mg mL^{-1} compared with 1.8 mg mL^{-1}. To clarify the nature of the interaction between the two matrix components, we measured surface dendrite growth on various matrix compositions over a broad range of collagen and IKVAV-PA concentrations (similar to PC survival experiments). Surface fitting of these sampled concentrations for surface area and convex hull revealed that surface dendrite growth was optimal for a narrow range of collagen to PA ratios (Fig. 4B). Remarkably, even though both high IKVAV-PA (with low collagen) and high collagen alone restricted surface growth, the combination of high IKVAV PA with high collagen produced the opposite effect.

PCs also demonstrated a concentration-dependent change for both collagen and IKVAV for substrate-penetrating dendrite growth. However, the response was distinct from the response of surface dendrites. Instead of having maximum penetration near a specific ratio of collagen and IKVAV PA, dendrite penetration was associated with either increasing PA concentration or decreasing collagen concentration in the hybrid matrix (Fig. 4A). Quantification of the substrate-penetrating growth by measuring the vertical span (the vertical distance between the top surface of the PC cell body to the tip of the dendrite showing maximum penetration) further supported this observation, demonstrating a 4-fold increase in the vertical span when the collagen concentration was changed from 6.0 mg mL^{-1} to 0.45 mg mL^{-1} (Fig. 4C), with a maximal depth reached of 60–70 μm at the lowest collagen concentration.

Since surface and substrate-penetrating dendrite growth are differentially regulated by matrix composition, we sought to better understand the relationship between these two types of growth. To compare the temporal course of their development, we analyzed PC dendrite morphology at 16 and 23 days *in vitro*, cultured on a matrix composition (collagen 1.8 mg mL^{-1}, IKVAV PA 1 mg mL^{-1}) that allowed both surface and substrate-penetrating growth. We observed a significant increase in both surface area and convex hull (increased by 43 ± 9% and 107 ± 18% respectively) during this time, while the substrate-penetrating growth showed some regression (−19 ± 4%) (Fig. 4D). This finding reveals that dendrite penetration, which is guided by high relative IKVAV-PA content, is restricted to the early phases of PC maturation, while dendrite surface extension, facilitated by the optimal collagen to PA ratio, continues as PCs mature in culture.

In these experiments, collagen and PA content in the hybrid matrix was varied in order to present the PCs with a different concentration and ratio of collagen and IKVAV epitope. However, changes to the matrix composition could also affect the matrix mechanical properties. A number of studies have demonstrated that the rigidity of microenvironment can strongly influence neuronal development. For example, the percentage of neurons in an embryonic cortical culture was increased when a soft substrate with stiffness matching that of native brain tissue was used.[42] Softer substrates have also been shown to expedite hippocampal neuron development and promote axon specification *in vitro*,[43,44] while a more rigid substrate favored an increase in dendrite number and branching.[45] Therefore we compared the mechanical properties of the hybrid gels using rheology to measure the storage modulus, G' and loss modulus, G'' (Fig. S3†). We prepared a series of gels with IKVAV PA concentration of 0–2.0 mg mL^{-1}, the concentration range used for cell experiments, and collagen concentration of either 1.8 mg mL^{-1} or 6.0 mg mL^{-1} for these measurements. For a fixed collagen concentration, the storage modulus (a measure of the elasticity) was mostly independent from IKVAV PA concentration. However, when the collagen concentration in the gel was raised from 1.8 mg mL^{-1} to 6.0 mg mL^{-1} the storage modulus substantially increased (0.14–0.44 KPa *vs.* 1.1–1.2 KPa, at an angular frequency of 10 s^{-1} and 0.1% strain). This suggests that the hybrid matrix stiffness is mainly determined by the collagen component. The IKVAV PA concentration, however, induced striking differences in PC density and surface dendrite growth. Since these gels would have similar storage moduli, this suggests a minimal influence of matrix rigidity on the phenotypic response observed from PC cultured on the hybrid matrix with varying IKVAV-PA. In contrast, an increased stiffness at higher collagen concentration could contribute to reduced substrate-penetrating growth, as neurite extension inside matrix is known to be inversely correlated with stiffness.[46]

Synaptic connectivity and spinogenesis on surface and substrate-penetrating dendrites

PC dendrites continue to grow until the end of the third week when cultured on glass coverslips, matching with the timeframe of maturation *in vivo*.[47,48] Afferent connectivity from GCs is known to exert a strong trophic influence in this growth process.[47,49] We therefore investigated whether the afferent connections also contribute to the maturation of PC surface and substrate-penetrating dendrites. The network activity of cerebellar neurons cultured on the hybrid matrix (collagen 1.8 mg mL^{-1}, IKVAV PA 1 mg mL^{-1}) was reduced by continuous exposure to a Na$^+$ channel blocker (tetrodotoxin, TTX, 1 μM), or was increased by exposure to an inhibitor of glutamate receptor desensitization (cyclothiazide, CTZ, 20 μM). Treatment with TTX for 16 days resulted in a decrease of PC cell surface area and convex hull by 27 ± 4% and 28 ± 7%, respectively, while CTZ treatment enhanced these parameters by 15 ± 4% and 31 ± 7% (Fig. 5). Both drugs induced a small reduction (10–12%) in the depth of dendritic substrate-penetration. These results suggest that synaptic activity promotes the growth of PC surface dendrites, although the amplitude of growth response is lower than ECM-mediated signaling. Moreover, the absence of activity-mediated effects on substrate-penetrating growth illustrates the locally restricted nature of such influence.

The differences in activity-mediated control over PC surface and substrate-penetrating dendrite development led us to probe whether these two forms of dendritic growth also
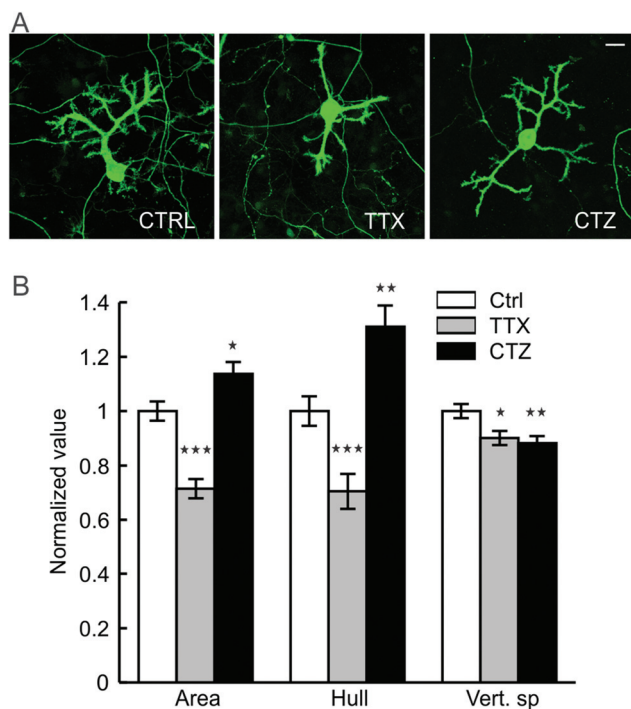
Fig. 5 Network activity and PC dendrite growth on hybrid matrix. (A) Representative micrographs of 16 days old PCs on hybrid matrix (collagen 1.8 mg mL^{-1}, PA 1 mg mL^{-1}) without any pharmacological treatment (control, left image) and in presence of tetrodotoxin (TTX 1 μM, middle image) or cyclothiazide (CTZ 20 μM, right image). Scale bar 20 micron. (B) Quantification of PC dendrite morphology following exposure to TTX and CTZ [*: $p < 0.05$, **: $p < 0.01$, ***: $p < 0.001$; $n > 100$ PCs].

differ in the formation of synaptic contacts with other neurons in culture. PCs are known to receive excitatory glutamatergic synaptic input through spines distributed on their dendrites. In culture on our hybrid matrix, both surface and substrate-penetrating dendrites had a high density of spiny protrusions (Fig. 6A). Staining with phalloidin demonstrated that these protrusions were rich in actin, an essential structural component of spine (Fig. 6B and C). However, a striking difference between the two types of dendrites was observed when stained for the pre-synaptic marker synaptophysin: synaptophysin staining was rarely observed around the spines of substrate-penetrating dendrites, while on surface dendrites, the spines were frequently associated with synaptophysin-positive punctae (Fig. 6A, inset). Association of synaptophysin punctae with the spines of surface dendrites suggests established contacts with axon terminals, presumably with GC axons, the only source of excitatory afferents in this culture.[49] Conversely, the absence of this pre-synaptic marker on spines of substrate-penetrating dendrites suggests that they do not make contact with the axon terminal. This finding was expected, as GC neurites were mainly distributed on the matrix surface (Fig. 6D), and PCs are known to form spines even in the absence of afferent axons.[23] However, we did find occasional apposition of synaptophysin puncta with PC spines (Fig. 6A, arrow in inset), indicating that these substrate-penetrating dendrites are capable of forming synaptic contact when a GC axon penetrates the substrate (Fig. 6D and E, arrow).
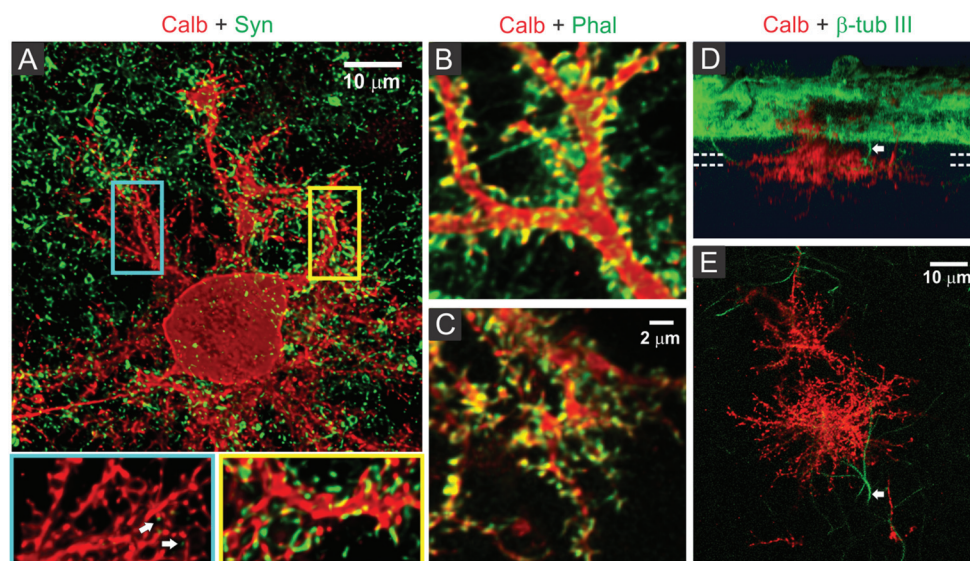

Fig. 6 Spine development and synaptic connectivity on PC dendrites. (A) Distribution of presynaptic terminals (synaptophysin, green) on PC dendrites (calbindin, red) in two weeks old culture on hybrid matrix (collagen 1.8 mg mL^{-1}, PA 1 mg mL^{-1}). Magnified views of segments from substrate-penetrating (blue rectangle) and surface dendrites (yellow rectangle) show the presence of numerous spiny protrusions, although the substrate-penetrating dendrites are only rarely associated with presynaptic terminals (white arrow). The spiny protrusions, however, are rich in actin (phalloidin staining) in both surface dendrites (B) and substrate-penetrating dendrites (C). (D) SFP (Simulated fluorescent process) rendered side-view of a confocal image stack showing occasional penetration of non-PC neurites (β-tubulin III+/calbindin−) inside the matrix. (E) Top projection view from a 6.5 μm thick slice volume (indicated by parallel dotted lines in D) captures one such non-PC neurite (arrow) in close proximity to the substrate-penetrating PC dendrites.

Discussion

We have illustrated the coordinated spatiotemporal expression of collagen and lam-1 in the developing rat cerebellum, and the relationship of these ECM components to PC migration and morphological maturation. To further characterize the function of this relationship *in vitro*, we used a synthetic artificial matrix that combined collagen with a lam-1-derived IKVAV epitope and demonstrated that these two ECM signals acted in a synergistic manner that was dependent on their ratio rather than their absolute concentration within the matrix.

While the expression of several forms of collagen and lam-1 in the developing cerebellum has been reported (CDT-DB and ref. 10), we show here the dynamics of their spatial distribution. We have shown that the orchestrated expression of collagen and lam-1 was closely associated with PCs development, namely migration, axon growth and dendrite maturation. The association of these two ECM signals was systematically studied using *in vitro* culture, on a synthetic hybrid matrix that enabled us to elucidate functional signaling synergies between these two components. For example, the observed migration of PCs at the forefront of the lam-1 gradient and their final positioning in a collagen-rich environment *in vivo* could be related to our findings *in vitro* of poor PC survival in the presence of high IKVAV concentration, and improvement at a specific ratio of collagen and IKVAV. Similarly, PC axonal growth towards higher IKVAV epitope density in the hybrid matrix correlates with the observed axonal extension to the lam-1 rich region in the cerebellar primordium. High lam-1 epitope concentration also induced substrate-penetrating dendrite growth inside the hybrid matrix, similar to the observation of early PC dendrite growth in the laminin-rich cerebellar tissue *in vivo*. These functions of lam-1 in PC migration and maturation are consistent with the reported disorganization and stunted dendrite growth of PCs in laminin α1 knockout mice.[13] In this context, it is interesting to note that lam-1 promotes the growth of both axons and dendrites while also facilitating their appropriate orientation in the cerebellar cortex due to a difference in the timeframe of PC axon and dendrite development (axonal growth begins well before dendrite growth). These findings support a simple model of synergistic influence between collagen and lam-1 signaling on the architecture of the developing cerebellum, as illustrated in Fig. 1H.

One of our most striking observations is that PC survival and maturation is highly sensitive to the ratio of collagen and IKVAV-PA in the hybrid matrix. Previous reports have demonstrated similar complex and non-additive responses from both neuron and non-neuronal cells to a matrix comprised of multiple ECM proteins or epitopes.[16,50] The complexity of ECM signaling stem from the large number of ECM protein isoforms, the large diversity in integrin and non-integrin receptors expressed by cells, and the ability of a number of integrin receptor subtypes to bind many ECM molecules.[51] For example, laminin and collagen are both recognized by integrin subtypes $\alpha_1\beta_1$, $\alpha_2\beta_1$ and $\alpha_{10}\beta_1$ and binding affinity depends on the specific laminin or collagen isoform.[52,53] Moreover,

integrin-mediated activation of cell signaling cascades and cytoskeletal response rely on ligand binding and receptor-clustering.[54] We speculate that the competitive binding of different ECM proteins to integrin receptors may provide a cell with more graded and specific information about its surrounding ECM environment. In this model, cells respond to the relative ratio of different ECM proteins in their immediate environment rather than to absolute concentrations. The benefit of relying on the ratio of ECM signals would be enhanced sensitivity of the cell to ECM, since substantial change in the ratio can be achieved quickly and easily if expression of each ECM change modestly but in opposite direction.

The three-dimensional matrix reported here for cerebellar culture allows for the study of two phenotypically distinct modes of dendritic growth that arise from PCs—surface growth at the matrix-media interface and substrate-penetrating growth into the matrix. Surface growth appears to follow a neurite growth model based on the adhesion strength to a substrate,[55] where a specific ratio of collagen to IKVAV-PA provides for optimal adhesion. In contrast, the increase in substrate-penetrating dendrites at higher PA concentrations suggests a guiding influence from the lam-1 derived IKVAV signal, possibly through activation of native ECM-specific cell signaling cascades. The reduced growth of substrate-penetrating dendrites, seen when the collagen concentration is increased, could be due to harder substrate created by higher matrix fiber density and stiffness,[56] as opposed to excessive surface adhesion. Additionally, substrate-penetrating dendrites demonstrated numerous spines, even in the absence of synaptic contacts. This observation supports the "Sotelo model" of PC spine development, which suggests that a cell-autonomous mechanism drives spine development in PCs.[57,58] Laminin is thought to play an important role in the process of spine formation,[12] and may correlate with an increased expression of β1 integrin in PCs during the period of synaptogenesis—independent of the formation of excitatory synaptic connections.[59] Interestingly, IKVAV epitopes on PA nanofibers have been shown to upregulate β1 integrin expression,[60] which could contribute to the formation of the large number of spines on substrate-penetrating dendrites in the studies performed here. Though our hybrid matrix culture model enables two distinct modes of PC dendrite growth *in vitro*, it is difficult to make similar observations for both modes of growth *in vivo*, since during the course of maturation the entire dendritic arbor receives a GC afferent. An *in vivo* analog to the substrate-penetrating dendrites observed on the hybrid matrix can be seen in GC-depleted mouse models, where the absence of glutamatergic afferent synapses results in substantially reduced PC dendrite growth, but with a maintenance of spines.[23,61]

The hybrid matrix approach demonstrated here provides a facile and controllable artificial environment that enables *in vitro* testing of the role of ECM signals on neuronal maturation. This strategy allowed us to probe the synergistic effects of two distinct ECM signals—collagen and laminin—over a

wide range of matrix composition. Previous studies were constrained by the formation of laminin aggregates within the collagen matrix when these two proteins were mixed.[28] In addition, it also enables these studies to be performed in a three-dimensional geometry, as opposed to similar studies where neurite growth is constrained to the surface of a coverslip. Though the short IKVAV epitope does not recapitulate all functions of the full lam-1 protein, this epitope has been tied specifically to much of the neuron-specific activity of the complete protein.[29,30] Similarly, even though we found collagen type II to be the abundant form of collagen expressed in the cerebellar tissue, type I collagen was chosen for its better gelation, ease of access and structural similarity to the fibrillar type II variety.[62,63] Though this approach allows creating side-by-side substrates of different compositions to examine neuronal response, the substrate composition is not easily altered during neuronal development *in vitro*, and it is therefore difficult to replicate the temporal matrix dynamics observed *in vivo*. Nonetheless, the hybrid matrix approach proved useful for a systematic study of matrix composition on PC organization and maturation, providing a better understanding of our *in vivo* observations.

Conclusions

Our work has revealed an orchestrated spatial and temporal distribution of collagen and lam-1 in the cerebellum during development. The use of an engineered synthetic hybrid matrix system, which afforded a systematic control over the presentation of collagen and a bioactive lam-1-derived signal, allowed us to investigate the functional role of the specific expression for these two ECM components. Specifically, our findings using this engineered matrix suggest the potential for synergistic activity between these ECM signals that governs the survival and morphological differentiation of developing PCs. These findings were specific to PCs, as GCs did not demonstrate the same responsiveness to the matrix, and further emphasize the importance of the surrounding ECM on cell-specific signal transduction. Our three-dimensional hybrid matrix culture model could serve as a useful tool to further identify interactions between these ECM components for other cell or tissue types, and could be modified to also include presentation of soluble growth factors that are important for the development of neuronal cells and organization of neuron networks. More broadly, this study demonstrates the potential application of engineered matrices to enable detailed and systematic evaluation of the effects of ECM on the development and function of native tissues.

Abbreviations

PC   Purkinje cell
GC   Granule cell
Lam-1   Laminin-1
PA   Peptide amphiphile
ECM   Extracellular Matrix
EGL   External germinal layer
IGL   Internal granular layer

References

1 T. Rozario and D. W. DeSimone, *Dev. Biol.*, 2010, **341**, 126–140.
2 L. F. Reichardt and K. J. Tomaselli, *Annu. Rev. Neurosci.*, 1991, **14**, 531–570.
3 K. A. Venstrom and L. F. Reichardt, *FASEB J.*, 1993, **7**, 996–1003.
4 A. Dityatev, C. I. Seidenbecher and M. Schachner, *Trends Neurosci.*, 2010, **33**, 503–512.
5 K. Broadie, S. Baumgartner and A. Prokop, *Dev. Neurobiol.*, 2011, **71**, 1102–1130.
6 M. E. Hatten, M. B. Furie and D. B. Rifkin, *J. Neurosci.*, 1982, **2**, 1195–1206.
7 S. Murase and Y. Hayashi, *J. Comp. Neurol.*, 1998, **397**, 199–212.
8 T. Miyata, K. Nakajima, K. Mikoshiba and M. Ogawa, *J. Neurosci.*, 1997, **17**, 3599–3609.
9 H. Colognato and P. D. Yurchenco, *Dev. Dyn.*, 2000, **218**, 213–234.
10 S. K. Powell, C. C. Williams, M. Nomizu, Y. Yamada and H. K. Kleinman, *J. Neurosci. Res.*, 1998, **54**, 233–247.
11 I. Selak, J. M. Foidart and G. Moonen, *Dev. Neurosci.*, 1985, **7**, 278–285.
12 F. J. Seil, *Brain Res.*, 1998, **795**, 112–120.
13 N. Ichikawa-Tomikawa, J. Ogawa, V. Douet, Z. Xu, Y. Kamikubo, T. Sakurai, S. Kohsaka, H. Chiba, N. Hattori, Y. Yamada and E. Arikawa-Hirasawa, *Matrix Biol.*, 2012, **31**, 17–28.
14 A. Sato, Y. Sekine, C. Saruta, H. Nishibe, N. Morita, Y. Sato, T. Sadakata, Y. Shinoda, T. Kojima and T. Furuichi, *Neural Netw.*, 2008, **21**, 1056–1069.
15 J. L. Duband and J. P. Thiery, *Development*, 1987, **101**, 461–478.
16 C. J. Flaim, D. Teng, S. Chien and S. N. Bhatia, *Stem Cell Dev.*, 2008, **17**, 29–39.
17 J. A. McDonald, D. G. Kelley and T. J. Broekelmann, *J. Cell Biol.*, 1982, **92**, 485–492.
18 M. J. Humphries, *J. Cell Sci.*, 1990, **97**(Pt 4), 585–592.

19 S. Sur, E. T. Pashuck, M. O. Guler, M. Ito, S. I. Stupp and T. Launey, *Biomaterials*, 2012, **33**, 545–555.

20 M. O. Guler, L. Hsu, S. Soukasene, D. A. Harrington, J. F. Hulvat and S. I. Stupp, *Biomacromolecules*, 2006, **7**, 1855–1863.

21 G. Chandrakasan, D. A. Torchia and K. A. Piez, *J. Biol. Chem.*, 1976, **251**, 6062–6067.

22 S. Furuya, A. Makino and Y. Hirabayashi, *Brain Res. Brain Res. Protoc.*, 1998, **3**, 192–198.

23 C. Sotelo, *Prog. Neurobiol.*, 2004, **72**, 295–339.

24 J. Altman and S. A. Bayer, *J. Comp. Neurol.*, 1985, **231**, 42–65.

25 A. Weyer and K. Schilling, *J. Neurosci. Res.*, 2003, **73**, 400–409.

26 K. S. Cheah, E. T. Lau, P. K. Au and P. P. Tam, *Development*, 1991, **111**, 945–953.

27 A. W. Leung, S. Y. Wong, D. Chan, P. P. Tam and K. S. Cheah, *Dev. Dyn.*, 2010, **239**, 2319–2329.

28 D. Guarnieri, S. S. Battista, A. Borzacchiello, L. Mayol, E. De Rosa, D. R. Keene, L. Muscariello, A. Barbarisi and P. A. Netti, *J. Mater. Sci. Mater. Med.*, 2007, **18**, 245–253.

29 K. Tashiro, G. C. Sephel, B. Weeks, M. Sasaki, G. R. Martin, H. K. Kleinman and Y. Yamada, *J. Biol. Chem.*, 1989, **264**, 16174–16182.

30 G. A. Silva, C. Czeisler, K. L. Niece, E. Beniash, D. A. Harrington, J. A. Kessler and S. I. Stupp, *Science*, 2004, **303**, 1352–1355.

31 J. D. Hartgerink, E. Beniash and S. I. Stupp, *Science*, 2001, **294**, 1684–1688.

32 J. D. Hartgerink, E. Beniash and S. I. Stupp, *Proc. Natl. Acad. Sci. U. S. A.*, 2002, **99**, 5133–5138.

33 H. Cui, M. J. Webber and S. I. Stupp, *Biopolymers*, 2010, **94**, 1–18.

34 J. B. Matson, R. H. Zha and S. I. Stupp, *Curr. Opin. Solid State Mater. Sci.*, 2011, **15**, 225–235.

35 H. Jiang, M. O. Guler and S. I. Stupp, *Soft Matter*, 2007, **3**, 454–462.

36 H. Storrie, M. O. Guler, S. N. Abu-Amara, T. Volberg, M. Rao, B. Geiger and S. I. Stupp, *Biomaterials*, 2007, **28**, 4608–4618.

37 M. O. Guler, S. Soukasene, J. F. Hulvat and S. I. Stupp, *Nano Lett.*, 2005, **5**, 249–252.

38 E. Agius, Y. Sagot, A. M. Duprat and P. Cochard, *Neuroscience*, 1996, **71**, 773–786.

39 H. J. Pulkkinen, V. Tiitu, P. Valonen, J. S. Jurvelin, M. J. Lammi and I. Kiviranta, *Osteoarthritis Cartilage*, 2010, **18**, 1077–1087.

40 J. M. Seyer, D. M. Brickley and M. J. Glimcher, *Calcif. Tissue Res.*, 1974, **17**, 25–41.

41 K. Wolf, M. Te Lindert, M. Krause, S. Alexander, J. Te Riet, A. L. Willis, R. M. Hoffman, C. G. Figdor, S. J. Weiss and P. Friedl, *J. Cell Biol.*, 2013, **201**, 1069–1084.

42 P. C. Georges, W. J. Miller, D. F. Meaney, E. S. Sawyer and P. A. Janmey, *Biophys. J.*, 2006, **90**, 3012–3018.

43 A. Kostic, J. Sap and M. P. Sheetz, *J. Cell Sci.*, 2007, **120**, 3895–3904.

44 S. Sur, C. J. Newcomb, M. J. Webber and S. I. Stupp, *Biomaterials*, 2013, **34**, 4749–4757.

45 M. L. Previtera, C. G. Langhammer and B. L. Firestein, *J. Biosci. Bioeng.*, 2010, **110**, 459–470.

46 A. P. Balgude, X. Yu, A. Szymanski and R. V. Bellamkonda, *Biomaterials*, 2001, **22**, 1077–1084.

47 C. A. Baptista, M. E. Hatten, R. Blazeski and C. A. Mason, *Neuron*, 1994, **12**, 243–260.

48 M. Tanaka, Y. Yanagawa, K. Obata and T. Marunouchi, *Neuroscience*, 2006, **141**, 663–674.

49 H. Hirai and T. Launey, *J. Neurosci.*, 2000, **20**, 5217–5224.

50 J. C. Schense, J. Bloch, P. Aebischer and J. A. Hubbell, *Nat. Biotechnol.*, 2000, **18**, 415–419.

51 Y. Takada, X. Ye and S. Simon, *Genome Biol.*, 2007, **8**, 215.

52 M. Tulla, O. T. Pentikainen, T. Viitasalo, J. Kapyla, U. Impola, P. Nykvist, L. Nissinen, M. S. Johnson and J. Heino, *J. Biol. Chem.*, 2001, **276**, 48206–48212.

53 M. Tulla, M. Lahti, J. S. Puranen, A. M. Brandt, J. Kapyla, A. Domogatskaya, T. A. Salminen, K. Tryggvason, M. S. Johnson and J. Heino, *Exp. Cell Res.*, 2008, **314**, 1734–1743.

54 S. Miyamoto, S. K. Akiyama and K. M. Yamada, *Science*, 1995, **267**, 883–885.

55 J. C. Schense and J. A. Hubbell, *J. Biol. Chem.*, 2000, **275**, 6813–6818.

56 R. K. Willits and S. L. Skornia, *J. Biomater. Sci., Polym. Ed.*, 2004, **15**, 1521–1531.

57 C. Sotelo, *Prog. Brain Res.*, 1978, **48**, 149–170.

58 R. Yuste and T. Bonhoeffer, *Nat. Rev. Neurosci.*, 2004, **5**, 24–34.

59 S. Murase and Y. Hayashi, *J. Comp. Neurol.*, 1996, **375**, 225–237.

60 M. Srikanth, S. Das, E. J. Berns, J. Kim, S. I. Stupp and J. A. Kessler, *Neuro Oncol.*, 2013, **15**, 319–329.

61 F. Metzger and J. P. Kapfhammer, *Cerebellum*, 2003, **2**, 206–214.

62 M. van der Rest and R. Garrone, *FASEB J.*, 1991, **5**, 2814–2823.

63 D. J. Hulmes, *J. Struct. Biol.*, 2002, **137**, 2–10.